©2004 IEEE. Personal use of this material is permitted. However, permission to reprint/republish this material for advertising or promotional purposes or for creating new collective works for resale or redistribution to servers or lists, or to reuse any copyrighted component of this work in other works must be obtained from the IEEE.

A SYMMETRIC ANALOGUE DEMODULATOR FOR OPTICAL FIBER INTERFEROMETRIC SENSORS

Charles B. Cameron, Robert M. Keolian, and Steven L. Garrett
Physics Department, Code PH/Gx, Naval Postgraduate School
Monterey, CA 93943-5000

ABSTRACT

This paper describes a form of passive homodyne demodulation for recovering a signal of interest from a Mach-Zender optical fiber interferometric sensor. The interferometer uses a 2×2 optical fiber coupler at the input, a push-pull arrangement to stretch the fibers comprising the two legs of the interferometer in a differential manner, and a 3×3 optical fiber coupler at the output, generating three phase-modulated outputs. The demodulator uses all three outputs in a symmetric manner to reconstruct the signal of interest. A dynamic range of 115 dB in a 1 Hz bandwidth has been measured for a circuit implementing this scheme. The minimum detectable signal at a frequency of 600 Hz is 220 μrad/√Hz. The maximum acceptable signal at 600 Hz is 140 rad and increases linearly with decreasing frequency.

BACKGROUND

Recently, optical fiber interferometric sensors of very high sensitivity have been reported.[1, 2, 3] These can now generate optical phase shifts of hundreds and thousands of radians. Earlier optical fiber interferometric sensors had generated phase shifts in the range of several μrad to around 1 rad. The goal in the research described in this paper was to find a technique for demodulating signals from this new class of push-pull optical fiber interferometric sensors.

To conduct the research, we built an interferometer in the lab which could generate phase shifts of up to 250 rad. These phase shifts were generated by voltage signals applied from a signal generator. In general, inteferometers to detect acoustic fields, magnetic fields, acceleration, seismic activity, and so on generate similar signals, and they all can be demodulated in the same manner.

CONSTRUCTION OF THE INTERFEROMETER

A schematic drawing of our interferometer is shown in Figure 1. It was constructed with 125 μm diameter, single-mode optical fibers. We inject coherent laser light from an 830 nm Sharp LT-015 laser diode into one leg of a 2×2 optical fiber coupler. The other input is unused. The two outputs of the 2×2 coupler comprise the two legs of a Mach-Zender interferometer. Each leg contains a piezo-electric cylinder. Application of a voltage signal to such a cylinder causes it to expand or contract, depending on the sign of the voltage. Each of the cylinders in our interferometer is connected to the same signal source, but with opposite polarity. Thus they operate in a differential (push-pull) manner, converting the signal of interest into strain of the optical fiber.

The resultant difference in optical path length induces a relative phase shift in the laser light in each leg. The two optical signals are injected into two of the three inputs of a 3×3 optical fiber coupler, where they interfere with one another. The third input is left unused. The three outputs of the 3×3 coupler produce signals which differ by 120° in phase.[4, 5, 6] If allowance is made for additional contributions $\phi(t)$ to the phase shift from pressure, temperature, and other factors, then we can describe the output u_k of leg k by the equation

$$u_k = D + E\cos\left[\xi(t) + \phi(t) - (k-1)\frac{2}{3}\pi\right]. \qquad (1)$$

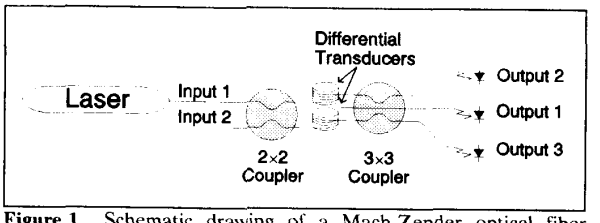

Figure 1 Schematic drawing of a Mach-Zender optical fiber interferometric sensor for detecting voltage signals.

In this expression, k can be 1, 2, or 3. For the moment, we shall neglect the "static" phase shift $\phi(t)$, regarding it as part of the signal of interest $\xi(t)$. D is the central value of the optical intensity emitted by the fibers. E is the peak change in intensity from this central value. The form of the three equations represented by this expression is given graphically in Figure 2 for the case where the signal of interest induces an optical phase shift

$$\xi(t) = A\sin(\omega t). \qquad (2)$$

This waveform is a pure sinusoidal function of time t with phase amplitude $A=5\pi$ and an unspecified frequency ω. The three interferometric outputs in the figure all look similar, but they represent signals with phase shifts 120° apart from each other. The three outputs are separated from each other vertically so that they can be seen individually, and the sinusoidal stimulus is superimposed on the plot (to a different scale) so that the relationship between the stimulus and the interferometric outputs can be readily observed.

SYMMETRIC DEMODULATION

Figure 8 at the end of this paper is a block diagram of the method of symmetric demodulation. The three interferometric optical signals are converted to voltage signals by photodiodes and low-noise transimpedance amplifiers. To eliminate the effects of fluctuations in D, we must first measure it. To do this, we first sum each of the three output signals u_k. The three cosine terms cancel,

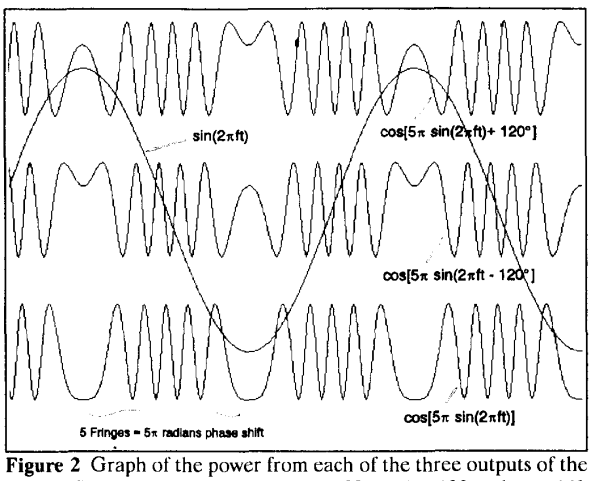

Figure 2 Graph of the power from each of the three outputs of the optical fiber interferometric sensor. Note the 120° phase shift between each leg.

91-645128/92$03.00 © 1992 IEEE

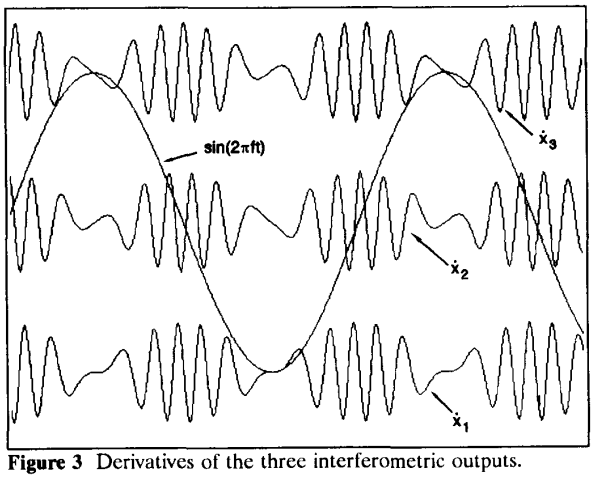

Figure 3 Derivatives of the three interferometric outputs.

and we are left with the sum $3D$. If we let the gain of the scaling, inverting adder which performs this addition be k_I=-1/3, then the sum is just $-D$.

This sum is added to each of the three interferometric outputs by adders with gain k_{A_1} to produce three scaled wave forms x_{kI}. These results each are differentiated by differentiators of gain k_D, yielding

$$k_D\dot{x}_k = -k_D k_{A_1} E\dot{\xi}\sin\left[\xi-(k-1)\frac{2}{3}\pi\right]. \tag{3}$$

The three derivatives are shown in the plots of Figure 3 for the same values of A and ω as in Figure 2. Again, the sinusoidal stimulus is shown for reference, although still not to the same vertical scale as the derivatives.

The next step in the processing is to take the difference between each of the three possible pairings of the derivatives and multiply this by the third signal (not differentiated). Let the gain of the multiplier be k_M. We start by combining signal x_1 with the derivatives of x_2 and x_3.

$$k_M x_1(\dot{x}_2-\dot{x}_3) = k_M k_{A_1} E\cos(\xi)\left[\begin{array}{c} -k_D k_{A_1} E\dot{\xi}\sin\left(\xi-\frac{2}{3}\pi\right) \\ +k_D k_{A_1} E\dot{\xi}\sin\left(\xi+\frac{2}{3}\pi\right)\end{array}\right]. \tag{4}$$

This simplifies to

$$k_M x_1(\dot{x}_2-\dot{x}_3) = k_M k_{A_1}^2 k_D E^2\,\dot{\xi}\cos(\xi)\left[\begin{array}{c} -\sin\left(\xi-\frac{2}{3}\pi\right) \\ +\sin\left(\xi+\frac{2}{3}\pi\right)\end{array}\right]. \tag{5}$$

We can apply to this the trigonometric identity

$$\sin(A+B)-\sin(A-B) = 2\cos(A)\sin(B) \tag{6}$$

and get

$$\begin{aligned} k_M x_1(\dot{x}_2-\dot{x}_3) &= k_M k_{A_1}^2 k_D E^2\,\dot{\xi}\cos(\xi)\left[2\cos(\xi)\sin\left(\frac{2}{3}\pi\right)\right] \\ &= \sqrt{3}k_M k_{A_1}^2 k_D E^2\,\dot{\xi}\cos^2(\xi). \end{aligned} \tag{7}$$

Using the same procedure we can combine signal x_2 with the derivatives of x_3 and x_1 and signal x_3 with the derivatives of x_1 and x_2, which yields

$$k_M x_2(\dot{x}_3-\dot{x}_1) = \sqrt{3}k_m k_{A_1}^2 k_D E^2\,\dot{\xi}\cos^2\left(\xi-\frac{2}{3}\pi\right) \tag{8}$$

and

$$k_M x_3(\dot{x}_1-\dot{x}_2) = \sqrt{3}k_m k_{A_1}^2 k_D E^2\,\dot{\xi}\cos^2\left(\xi+\frac{2}{3}\pi\right). \tag{9}$$

Equations (7), (8), and (9) are depicted in Figure 4. Once again, we include the sinusoidal stimulus. Note that the envelope of the three signals is itself now sinusoidal.

To extract the envelope, we sum the three expressions of Equations (7), (8), and (9), using the gain constant k_{A_3}, and obtain

$$\begin{aligned} &\sqrt{3}k_{A_3} k_M k_{A_1}^2 k_D E^2\,\dot{\xi}\left[\cos^2(\xi)+\cos^2\left(\xi-\frac{2}{3}\pi\right)+\cos^2\left(\xi+\frac{2}{3}\pi\right)\right] \\ &= \frac{3}{2}\sqrt{3}k_{A_3} k_M k_{A_1}^2 k_D E^2\,\dot{\xi}. \end{aligned} \tag{10}$$

We have applied here the identity

$$\sum_{k=0}^{N-1}\cos^2\left(\phi+\frac{k2\pi}{N}\right) = \frac{N}{2} \tag{11}$$

with N=3.

In Figure 5 we illustrate the result of the summation for the example we have been using throughout, in which the amplitude of the stimulus is $A=5\pi$ radians. It should be clear from the figure that the sum of products is indeed proportional to the derivative of the sinusoid displayed with it. In the figure, the amplitudes of each waveform have been scaled for convenience.

If we wanted to, we could simply integrate the expression in Equation (10) and get a fair replica of the original signal of interest, $\xi(t)$. However, there is a factor of E^2 in the expression, which implies that the derivative still depends on the contrast between the dark and light extrema of the interference pattern. Since this is a number which wanders due to changes in laser intensity, temperature, and the polarization angle of the light within the optical fiber interferometric sensor, it would be useful to eliminate this factor.

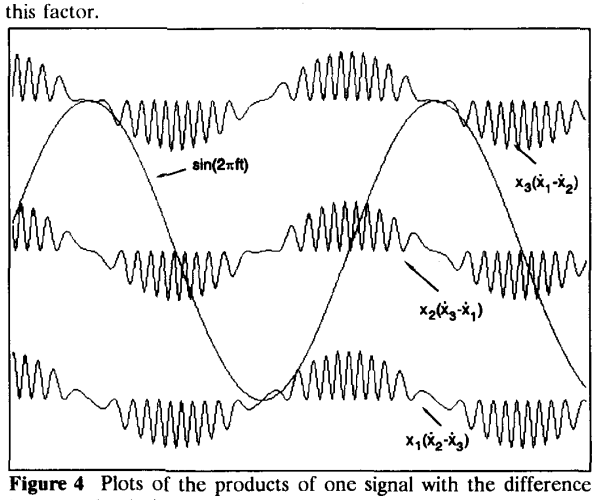

Figure 4 Plots of the products of one signal with the difference between the derivatives of the other two signals.

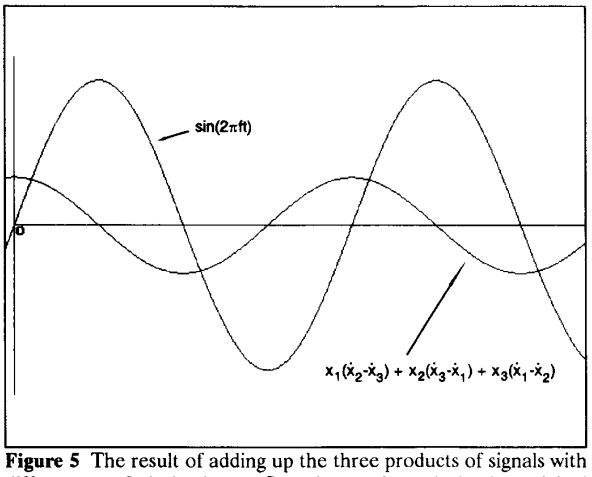

Figure 5 The result of adding up the three products of signals with differences of derivatives. Superimposed on it is the original stimulus of amplitude $A=5\pi$ radians.

We can find E^2 by squaring each of the signals x_k and adding them up. The squaring operation can be performed with another multiplier of gain k_M and the addition can be performed with another adder of gain k_{A_2}. That is

$$k_{A_2}\sum_{k=1}^{3} k_M\left\{k_{A_1}E\cos\left[\xi-(k-1)\frac{2}{3}\pi\right]\right\}^2 = \frac{3}{2}k_{A_2}k_m k_{A_1}^2 E^2. \qquad (12)$$

We have again applied Equation (11) in computing the sum.

Both Equations (10) and (12) include the factor E^2. We can eliminate this factor by dividing Equation (12) into Equation (10). Any practical divider has a gain which we shall call k_d (not to be confused with k_D, the gain of the differentiators discussed above.) Division yields

$$\frac{\sqrt{3}k_{A_3}k_D k_d}{k_{A_2}}\dot{\xi}. \qquad (13)$$

We can integrate this with an integrator of gain k_I to obtain

$$\frac{\sqrt{3}k_I k_{A_3}k_D k_d}{k_{A_2}}\xi. \qquad (14)$$

This completes our development of the method of symmetric demodulation of phase-modulated outputs of optical fiber interferometric sensors terminated with 3×3 optical fiber couplers. By the processing algorithm developed here, we have the ability to recover a scalar multiple of the signal of interest, $\xi(t)$. The dependence on D and E, which vary and so cause the interferometric outputs to wander, is eliminated. The scaling factor consists of constants which we can set in implementing the algorithm. They include the gains of two adders, the gain of three identical differentiators, and the gain of the final integrator. These factors can be chosen within certain constraints to provide $\xi(t)$ scaled to whatever level is desired. In an analogue implementation of this scheme, clipping of signals constrains the selection of these parameters at the high-frequency limit, and the noise of the circuit constrains their selection at the low-frequency limit.

ANALOGUE IMPLEMENTATION

In Figure 9 is a schematic drawing of the circuit used to implement the symmetric demodulation algorithm derived in the previous section. The three inputs are shown at the left hand side where three photodiodes convert the interferometric outputs into current signals. These currents are converted to voltage signals by three transimpedance amplifiers built around operational amplifiers U1, U2, and U3. The summation of the three voltage signals to compute D in Equation (1) is performed by the inverting summing amplifier built around operational amplifier U4A. This sum is subtracted from the outputs of the transimpedance amplifiers by operational amplifiers U5A, U6A, and U7A, whose outputs are described by

$$x_k = E\cos\left[\xi(t)+\phi(t)-(k-1)\frac{2}{3}\pi\right]. \qquad (15)$$

The derivatives are computed by differentiators built around operational amplifiers U5B, U6B, and U7B. The Analog Devices AD534 Multipliers U11, U12, and U13 have differential inputs. We apply one signal and a ground to one differential input in each. To the other, we apply the derivatives of the other two signals according to Equations (7), (8), and (9). Each signal is multiplied internally by the difference between the two derivatives of the other two signals. These three outputs are added in the inverting adder built around operational amplifier U14A to yield the result modelled in Equation (10). In order to remove the factor of E^2 in this result, another expression with E^2 in it is computed by the inverting adder built around operational amplifier U4B, which gets its own input from three more AD534 Multipliers, U8, U9, and U10. These multipliers are configured to square their inputs, which are the interferometric outputs stripped of D. The sum of these squares is of the form given in Equation (12). The Burr-Brown DIV100 Divider U15 takes the ratio of the output of U14A and that of U4B. This result is proportional to the derivative of the signal of interest, but without dependence on D or E, as shown in Equation (13). The final step in the circuit is to reconstruct from this the signal of interest shown in Equation (14). The integration is performed by the integrator built around operational amplifier U14B.

MEASURED PERFORMANCE

We measured several characteristics of the performance of the Symmetric Analogue Demodulator. These included scale factor, small-signal bandwidth, maximum acceptable signal, noise floor, dynamic range, complexity, and cost.

Scale Factor

The scale factor F_D (in V/rad) relates the output of the demodulator (measured in volts) to the input (measured in radians of optical phase shift). To measure the scale factor, we applied the output of an HP3314A Function Generator to a Gertsch Model 480 Ratio Standard. This permitted accurate test signals of low amplitude to be applied to the inputs of three Analogue Interferometric Simulators as shown in Figure 6. These simulators use an Analog Devices AD639 Universal Trigonometric Function Converter to create facsimiles of the output of the photodiodes in the receiver of an interferometer. By using them, we avoid the noise associated with a laser, and we can make measurements with constant values of D and E. The inputs to the receivers must be modified slightly to convert the voltage signal from the simulators to a current through a resistor. Thenceforth, the processing is identical to that of real interferometric outputs.

We used an EG&G Princeton Applied Research Model 5210 Lock-In Amplifier to make measurements of the outputs of the demodulator. We fed the output of the lock-in amplifier to an HP3456A Digital Voltmeter, which averaged the lock-in amplifier's output.

The scale factor F_D is approximately 31 mV/rad, compared to 29 mV/rad predicted from Equation (14). The close agreement between theory and observation is good evidence for the correctness of the theory. When the multiplicative product of signal amplitude and frequency is too small, the outputs of the differentiators become buried in noise and so the demodulator's output ceases to be proportional to the signal of interest. Similarly, when the product of the two is too big, saturation of the outputs of various components within the demodulator occurs, and so the circuit's output again ceases to be proportional to the signal of interest.

Small-signal Bandwidth

An optical fiber interferometric sensor is a non-linear system, and it creates many output frequencies for a single input frequency. Similarly, the Symmetric Analogue Demodulator is a non-linear system, capable of generating a single output frequency from a multiplicity of input frequencies. In the small-signal regime, however, both devices are not too unlike linear systems in that the fundamental frequency is dominant over all the harmonic overtones. The smaller the amplitude A of the signal of interest becomes, the more accurate this statement becomes.

These conditions guided our selection of the analogue electronic simulators rather than the optical interferometer to provide test inputs to the demodulator. They have a separate input to which a voltage dictating the "static" phase ϕ can be provided, in addition to the usual input to which a voltage dictating the phase amplitude A can be given. The value of the central value D of the interferometric output can be set to zero by adjustment of the DC offset on the front panel of the simulator. The level of the deviation E from D also can be controlled easily. The effect of these settings, provided A is small enough, is to change the interferometric signal to the simple form:

$$x(t) \approx -2E\, J_1(A)\, \cos(\omega t). \qquad \textbf{(16)}$$

$J_1(A)$ is the Bessel function of order one dependent on the signal amplitude A. We measured the small-signal bandwidth of the analogue electronic simulators to be about 1 MHz.

By this method, we could vary ω and so determine the small-signal bandwidth by finding the frequency f_{UPPER} where the scale factor decreases by $1/\sqrt{2}$. We found that the small signal bandwidth was 113 kHz.

Maximum Acceptable Signal

We defined the maximum acceptable signal as that which created a total harmonic distortion in the output of 4%. This level of distortion in a sine wave is barely perceptible, visually. We used an HP3561A Dynamic Signal Analyzer to perform the measurement of total harmonic distortion. For each of several frequencies we found the input phase amplitude required to exceed the 4% level. The data are represented in the upper curve in Figure 7.

There are two distinct regions to the graph. For frequencies of up to about 300 Hz, the graph is horizontal. This reflects a limitation on the peak phase shift we could achieve through the use of the HP6824A Power Amplifier, which saturated at around 60 V, to about 250 radians.

For frequencies above about 300 Hz the graph begins to fall at roughly 20 dB per decade of frequency. This appears to be a linear decline on a log-log plot and is a rectangular hyperbola on a linear-linear plot. It is the product of phase shift and frequency, the phase rate, which is crucial to the correct operation of the Symmetric Analogue Demodulator. This product cannot exceed a value which is approximately constant over the range in which the demodulator operates with constant scale factor. For our demodulator, the maximum phase rate Af is 65 krad/s.

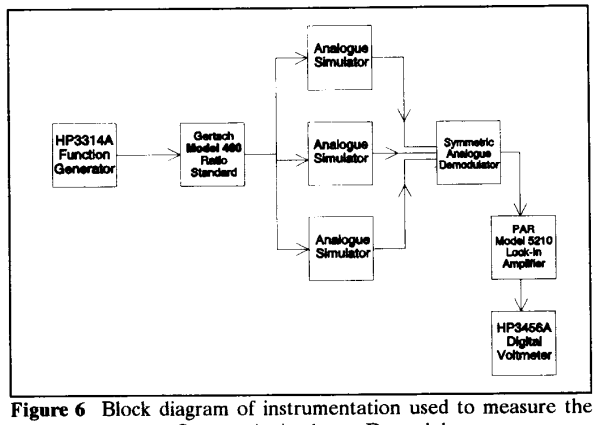

Figure 6 Block diagram of instrumentation used to measure the scale factor of the Symmetric Analogue Demodulator.

Noise Floor

We used a lock-in amplifier to measure the noise floor of the demodulator when its inputs were provided by the Analogue Interferometric Simulators mentioned earlier. Input signal amplitudes of decreasing levels were applied to the interferometer and the ratio of signal to noise was measured. This was extrapolated to find the level of signal which would make the signal equal to the noise.

The lower curve in Figure 7 summarizes the measured noise floor of the demodulator. Note that the spectral density is not constant with frequency, as it would be if it were white noise. Instead, it declines at the rate of about 20 dB per decade of increase in frequency, *i.e.*, the noise voltage spectral density is proportional to the reciprocal of the frequency, $1/f$. Consequently, its noise power spectral density declines at a rate proportional to $1/f^2$.

Dynamic Range

The ratio of the maximum acceptable signal to the noise floor is the dynamic range. Since the noise floor is given in a 1 Hz bandwidth, so is the dynamic range. A logarithmic plot of the upper and lower ends of the dynamic range is given in Figure 7. When the maximum acceptable signal begins its descent, both the upper and the lower limits decline at the rate of about 20 dB per decade of frequency increase. In this region, the dynamic range is 115 dB.

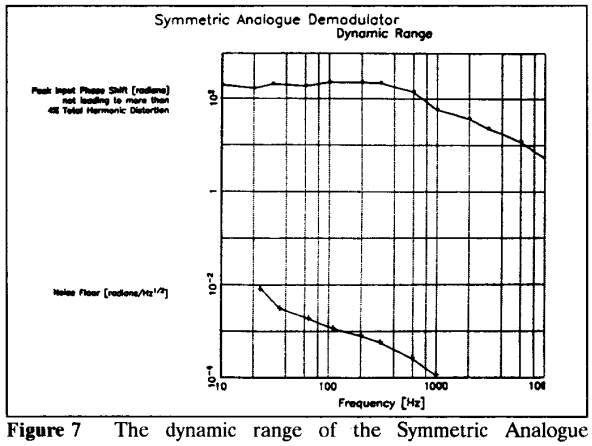

Figure 7 The dynamic range of the Symmetric Analogue Demodulator when the output is viewed in a 1 Hz bandwidth.

Complexity

The Symmetric Analogue Demodulator is of only moderate complexity. The chief difficulty is understanding the principles of its operation. This is essentially just an exercise in mathematics. Of course, the beauty of the mathematical models is not entirely matched by that of the real signals. They are noisy; those of the models have no noise. More significantly, the models we have used, those on which the algorithm are based, assume that all three outputs of the 3×3 coupler have the same constant offset D and the same amplitude E. In reality, these assumptions are more or less wrong. Despite this fact, the demodulator works quite well.

As far as the circuit itself is concerned, it does not consist of very many parts. It could be integrated onto a single (or possibly a very few) application-specific integrated circuits (ASIC) for some reduction in the amount of space, weight, and power required. As it is, it could fit onto a single printed circuit board without much difficulty.

Cost

The total cost of integrated circuits in this demodulator is $270. This price is very modest for a demodulator with 115 dB dynamic range, extending from hundreds of microradians to hundreds of whole radians. A practical demodulator would include some additional items, such as the printed circuit board, power supply, passive components, connectors, packaging, and the like.

Subsequent to the construction of this demodulator, Analogue Devices released the AD734 integrated circuit multiplier. At $14.77 each (in quantities of one), it is cheaper than the AD534 at $29.95 by a factor of 2. Its bandwidth is 10 MHz, versus 1 MHz for the AD534. Finally, its scale factor is programmable, whereas on the AD534 it is essentially fixed. This change lets the new chip perform division as well as multiplication. If it were used, the DIV100 chip used in our demodulator could be replaced by this new device. This substitution would lower the price to about $157 and increase performance.

CONCLUSION

For under $300.00 in parts, we have implemented a new kind of passive homodyne optical fiber interferometric sensor demodulation scheme. The new technique, which we call symmetric demodulation, can yield a large dynamic range, with phase amplitudes spanning the range between milli-radians and hundreds of radians. All three outputs of the interferometer are treated in a similar manner, and none is discarded, as in other passive homodyne demodulation schemes based on the use of 3×3 optical fiber couplers.[7] Because large phase amplitudes can be demodulated with this scheme, large dynamic range is available without the need for elaborate noise-reduction techniques and costly lasers which require wavelength modulation. The result of this is an inexpensive, capable demodulator of low complexity.

ACKNOWLEDGEMENTS

This work was supported by the Naval Sea Systems Command and the Naval Postgraduate School Direct Funded Research Program.

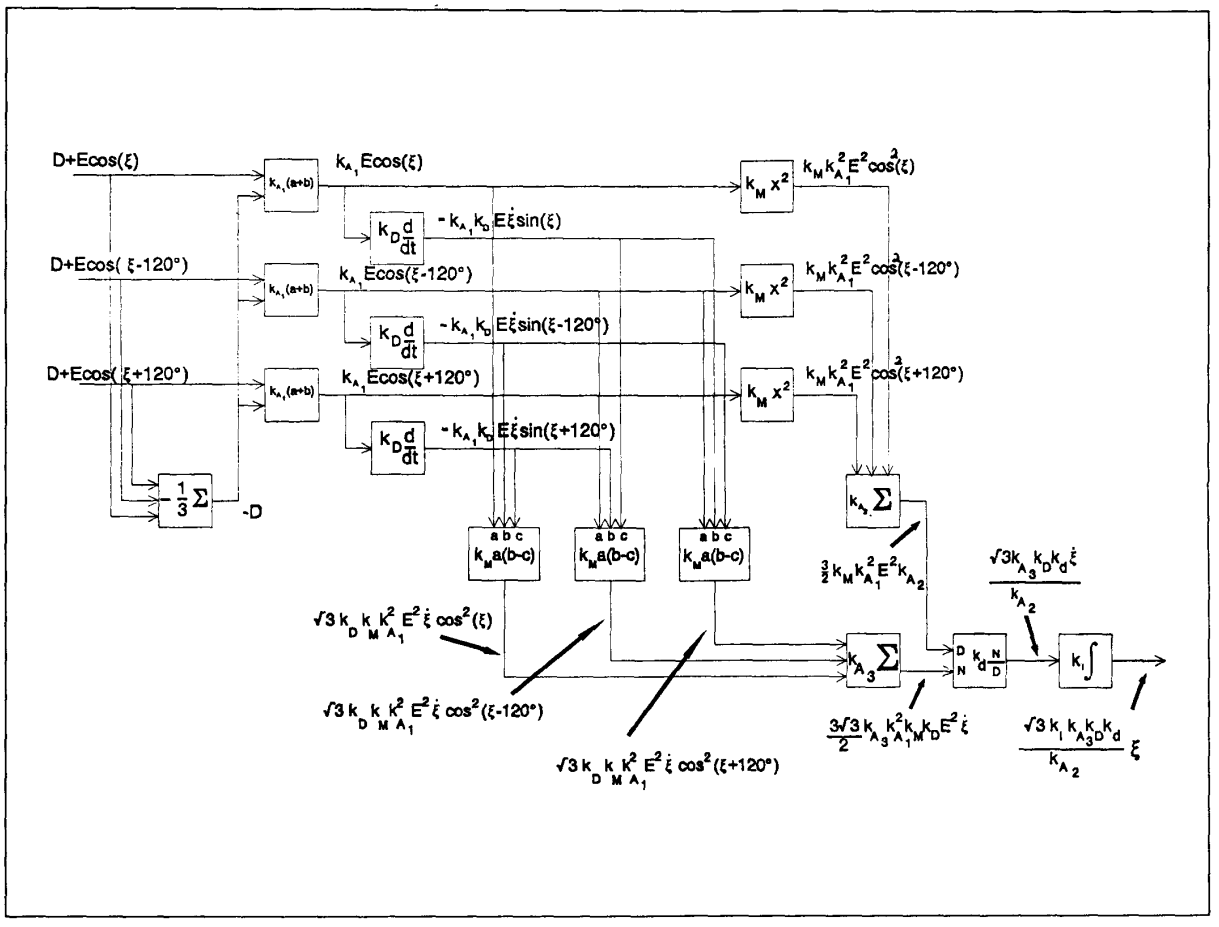

Figure 8 Block diagram of symmetric demodulation.

REFERENCES

1. D. L. Gardner and S. L. Garrett, "Fiber optic seismic sensor", *Fiber Optic and Laser Sensors V*, Proc. Soc. Photo-Optical Inst. Eng. (SPIE), **838** , 271-278 (1987); S. L. Garrett and D. L. Gardner, "Multiple axis fiber optic interferometric seismic sensor", U. S. Pat. No. 4,893,930 (Jan. 16, 1990).

2. D. A. Danielson and S. L. Garrett, "Fiber optic ellipsoidal flextensional hydrophones", J. Lightwave Tech. **LT-7**(12), 1995-2002 (1989); S. L. Garrett and D. A. Danielson, "Flextensional hydrophone", U. S. Pat. No. 4,951,271 (Aug. 21, 1990).

3. S. L. Garrett, D. A. Brown, B. L. Beaton, K. Wetterskog, and J. Serocki, "A general purpose fiber-optic interferometric hydrophone made of castable epoxy", *Fiber Optic and Laser Sensors VIII*, Proc. Soc. Photo-Optical Inst. Eng. (SPIE) **1367**, 13-29 (1990); T. Hofler and S. L. Garrett, "Flexural disk fiber optic hydrophone", U. S. Pat. No. 4,959,539 (Sept. 25, 1990).

4. S. K. Sheem, "Fiber-optic gyroscope with [3×3] directional coupler", *Applied Physics Letters*, Volume 37, Number 10, pp. 869-871, 15 November, 1980.

5. S. K. Sheem, "Optical fiber interferometers with [3×3] directional couplers: Analysis", *Journal of Applied Physics*, Volume 52, Number 6, pp. 3865-3872, June, 1981.

6. S. K. Sheem, *et al.*, "Optical Techniques to Solve the Signal Fading Problem in Fiber Interferometers", *Applied Optics*, Volume 21, Number 4, 689-693, 1982.

7. K. P. Koo, A. B. Tveten, and A. Dandridge, "Passive stabilization scheme for fiber interferometers using (3×3) fiber directional couplers", Appl. Phys. Lett. **41**(7), 616-618.

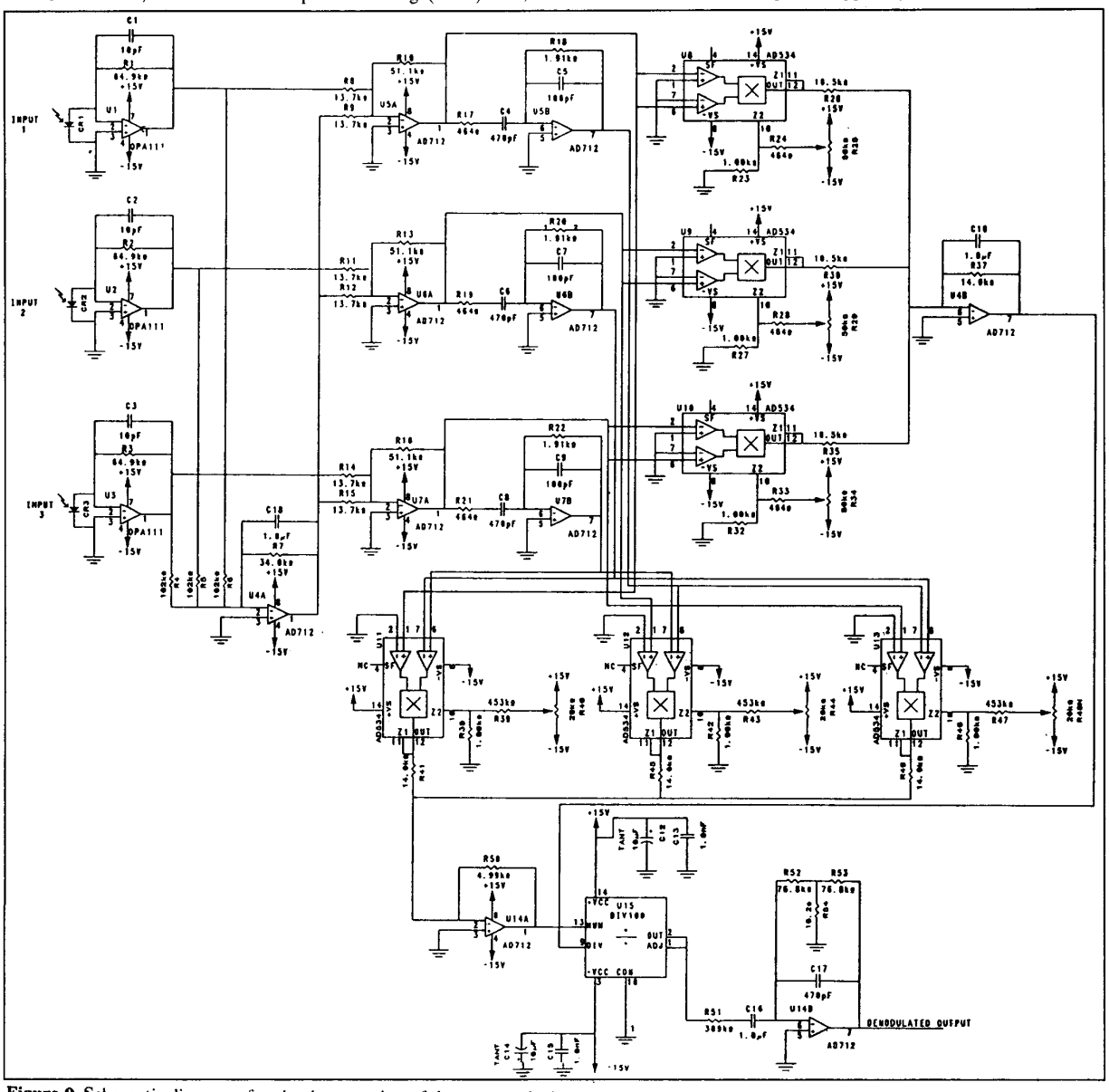

Figure 9 Schematic diagram of an implementation of the symmetric demodulation technique in analogue electronics.